Regulating bacterial dynamics by lime addition to enhance kitchen waste composting

Zhicheng Xu [a], Chuanren Qi [a], Lanxia Zhang [a], Yu Ma [a], Guoxue Li [a], Long D. Nghiem [b], Wenhai Luo [a] *

[a] *Beijing Key Laboratory of Farmland Soil Pollution Prevention and Remediation, College of Resources and Environmental Sciences, China Agricultural University, Beijing, 100193, China*

[b] *Centre for Technology in Water and Wastewater, School of Civil and Environmental Engineering, University of Technology Sydney, Ultimo, NSW 2007, Australia*

* Corresponding author: luowenhai@cau.edu.cn; Ph: +86 18311430503.

Abstract

This study examined bacterial dynamics in response to lime addition to enhance kitchen waste composting using modular network analysis. Bacterial communities could be separated into three meta-modules corresponding to the mesophilic, thermophilic, and mature stage of composting. Lime addition at 1% (wet weight) suppressed acidogens and denitrifiers (e.g. *Lactobacillus* and *Acinetobacter*) at the mesophilic stage to reduce greenhouse gas emissions. The matrix pH and temperature were also increased by lime addition via hydrogen reaction to favor bacterial growth and activity. Thus, thermophilic bacteria (e.g. *Thermoactinomycetaceae* and *Planifilum*) were enriched with lime addition to facilitate lignocellulose biodegradation for humus formation at the thermophilic stage. Further lime addition to 1.5% reduced ammonia emission at the thermophilic stage via chemical fixation. Moreover, lime inhibited denitrifiers but proliferated nitrifiers at the mature stage to decrease nitrous oxide emission and enhance nitrate content, respectively. As such, lime addition improved both biotic and abiotic composting performance.

Keywords: Kitchen waste composting, lime, modular network analysis, bacterial community.

1. Introduction

Rapid economic development and population growth as well as heightening concern over resource depletion and global warming have placed a spot light on food waste. According to the Food and Agricultural Organization of the United Nations (FAO), globally 1.3 billion tons of food waste is generated each year. The disposal of food waste in landfills entailed many environmental consequences especially greenhouse gas (GHG) emission from the degradation of organic materials. Progressive actions to address the problem of food waste have been taken by authorities around the world. Many European countries have banned the disposal of food waste by landfilling (Nghiem et al., 2017). Australia has set a national target to half the amount of organic waste in landfill by 2030. In April 2021, China has enacted new legislation to prevent food wastage and foster a “resource conserving” society. It is also recognized that a large fraction of food waste is unavoidable. This includes kitchen waste such as banana peel, fruit husks, inedible animal products (e.g. skin, bone, and offal) from food processing and meal preparation. Kitchen waste has a high moisture content and is highly putrescible (Cheng et al., 2020). Thus, the excessive accumulation of kitchen waste or improper disposal can severely deteriorate environmental issues by releasing leachate, generating offensive odors, and proliferating pathogens (Xiong et al., 2019). Kitchen waste, on the other hand, is a valuable resource that can be transformed into biofertilisers and biofuel via several advanced biotechnologies to achieve sustainable development (Yang et al., 2019).

Aerobic composting has been verified to effectively convert kitchen waste into high-quality organic fertiliser. In general, kitchen waste composting alone cannot achieve compost maturity, given its unfavorable physiochemical properties, including compact structure, high moisture content, and low matrix pH (Yang et al., 2013). Thus, several pragmatic approaches, such as adding bulking agents and improving operational parameters, have been reported to improve kitchen waste composting from the perspectives of humification and gaseous emissions (Ding et al., 2019; Xu et al., 2021c). Despite their potential for composting performance, these strategies hardly improve acidification characteristic of kitchen waste caused by anaerobic acidogens during storage and transportation. The acidification of kitchen waste could inhibit the metabolisms of aerobic microbes to favor the proliferation of anaerobes, thus, delaying temperature increase and humification as well as exacerbating GHG and malodour emissions during composting (Xu et al., 2021a). Nevertheless, to date, no relevant studies have been dedicated to the development of countermeasures to further ameliorate kitchen waste composting.

Lime, which is a calcium containing mineral composed primarily of calcium oxide (CaO), has been widely implemented for acidic soil amelioration (Wang et al., 2021b). Previous studies have evidenced that the addition of lime into acidic soil could significantly increase crop yields and soil organic carbon stocks by enhancing soil pH to optimize microbial diversity and its composition (Li et al., 2019b). In addition, methanotrophic activities and plant nitrogen uptake could also be enhanced with lime addition to control soil GHG emission (Wang et al., 2021b). On the other hand, lime has also been employed in composting of livestock manure or sewage sludge to immobilize toxic heavy metals, disinfect pathogens, and improve humification (Singh & Kalamdhad, 2013; Chen et al., 2021). Singh and Kalamdhad (2013) reported that lime addition decreased water soluble and plant-available heavy metals (including cadmium and lead) to undetectable level during co-composting of cattle manure and water hyacinth. Despite these advantages of lime amelioration, the performance and mechanisms of lime addition to regulate physiochemical characteristics and bacterial dynamics for advanced kitchen waste composting have not been systematically elucidated.

High-throughput sequencing technology has been extensively applied to determine the bacterial composition and succession in composting (Zhao et al., 2019). Previous studies have observed remarkable bacterial shifts during composting due to bacterial interactions to alter temperature and substrate components (Wei et al., 2018; Xu et al., 2021c). Nevertheless, recent studies have concentrated mostly on the dominant taxa during composting, which cannot fully reflect the interaction patterns in the bacteria communities and their response to environmental factors (Liu et al., 2018; Wei et al., 2018; Yin et al., 2019). As inspired by previous studies on soil microbial community (Deng et al., 2012; Fernandez-Gonzalez et al., 2020), modular network analysis could be considered as a pragmatic strategy to expand bacterial community analysis. Such network gathers bacteria that have similar ecological functions into identical modules, which then can be used to determine their responses to varying environmental conditions. For instance, Jiang et al. (2015) used modular network analysis to reveal that soil pH and total carbon could significantly enhance the interactions between nematodes and ammonia oxidizers to improve soil nitrogen cycling. However, the application of modular network analysis to decipher microbial dynamics in composting is still limited.

This study aims to reveal the performance and mechanisms of lime addition to regulate bacterial dynamics for advanced kitchen waste composting using modular network analysis. Humification and gaseous emissions were determined to evaluate composting performance. Modular network analysis was then conducted to decipher the succession of bacteria communities and identify key functional bacteria for lignocellulose degradation, humification and gaseous emissions. Results reported here will provide valuable understanding on the performance of lime addition to improve kitchen waste composting.

2. Materials and methods

2.1 Composting materials

Fresh kitchen waste was from a local solid waste collection station (Beijing, China). The kitchen waste contained 40.2% vegetables, 28.7% fruits, 15.2% staple food, 5.1% meat, 5.0% bones, and 5.8% unclassified materials based on their wet weight. The unclassified fraction is likely to be a combination of putrescible materials such as vegetables, fruits, and meats but could not be clearly identified due to rapid degradation during collection, transportation and storage. Garden waste was provided by a landscape company (Jiangsu, China) and used as the bulking agent for kitchen waste composting. The garden waste was air-dried to achieve less than 5% moisture content and then mechanically cut to the length of 2 – 4 cm. Kitchen and garden wastes were co-composted at the wet weight ratio of 17:3. This ratio could effectively facilitate organic biodegradation and reduce gaseous emission to advance kitchen waste composting (Xu et al., 2021a). Key physiochemical characteristics of these composting materials were summarized in Table 1. Lime with more than 95% CaO content was used to amend composting performance.

Table 1: Key physiochemical characteristics of composting materials (mean value ± standard deviation from triplicate measurements). Kitchen and garden wastes were mixed at the mass ratio of 17:3. # denotes parameters that were determined based on the dry mass.

Parameters	Kitchen waste	Garden waste	Mixture
pH	4.7 ± 0.1	7.2 ± 0.1	5.0 ± 0.1
Electrical conductivity (mS/cm)	2.1 ± 0.2	1.2 ± 0.1	1.5 ± 0.1
Moisture content (%)	72.8 ± 3.4	4.9 ± 1.2	66.8 ± 1.7
Total carbon (%) #	37.6 ± 0.8	41.2 ± 0.3	38.5 ± 0.2
Total nitrogen (%) #	2.4 ± 0.1	0.56 ± 0.1	1.64 ± 0.1
Total sulphur (%) #	0.57 ± 0.1	0.14 ± 0.1	0.41 ± 0.1
Carbon/nitrogen ratio #	15.6 ± 0.3	73.5 ± 0.1	24.0 ± 0.2
Ammonium nitrogen ($g \cdot kg^{-1}$) #	1.6 ± 0.3	0.33 ± 0.1	1.39 ± 0.1
Nitrate nitrogen ($g \cdot kg^{-1}$) #	1.3 ± 0.3	0.12 ± 0.1	1.12 ± 0.2

2.2 Experimental system and protocols

A bench-scale composting system (consisting of multiple 60 L cylindrical composters, rod-shaped temperature sensors, and an automatic aeration device) was employed in this study. The details of this system have been described in our previous study (Xu et al., 2021c). Briefly, each composter with a detachable lid was made of double-layers stainless steel for heat conversation. Two holes designed in the detachable lid were used to insert temperature sensor and capture released gases from the composter for further measurement, respectively. All temperature sensors were wirelessly connected with a computer for temperature recording. The automatic aeration device was used to provide a continuous aeration of 0.36 L kg $^{-1}$ dry mass min $^{-1}$ from the composter bottom. To ensure homogenous air diffusion to composting piles, a stainless-steel plate with evenly distributed holes was placed at the composter bottom.

Four treatments (denoted T1 to T4) were conducted in parallel under identical condition over 5 weeks with the exception of lime addition dosage. "T1 (0%)" is the control treatment without any lime addition. Lime was added to the composting materials on dry mass basis at 0.5%, 1%, and 1.5% corresponding to "T2 (0.5%)", "T3 (1.0%)", and "T4 (1.5%)", respectively. Manual turning and then compost sampling were conducted on day 3 and 7 in the first week and then once per week. Fresh compost samples were preserved at -80 °C for bacterial analysis. Moreover, certain fresh samples were air-dried for subsequent analysis of physiochemical properties, lignocellulose degradation, and humification characteristics. Released gases from the composters were captured daily for analysing gaseous emissions.

2.3 Analytic methods

2.3.1 Gaseous emissions and physiochemical properties

Gaseous emissions were evaluated by monitoring carbon dioxide (CO_2), methane (CH_4), nitrous oxide (N_2O), and ammonia (NH_3) in the off gas. CO_2 was measured by a potable biogas detector (Biogas-5000, Geotech, UK). CH_4 and N_2O were sampled using syringe and then quantified by a gas chromatograph (Beifen, China). NH_3 was examined by 2% boric acid absorption and then titration against 0.1 M sulphuric acid.

Water and potassium chloride (KCl) extracts were obtained by completely mixing fresh compost samples with deionized water and 2 M KCl at a mass ratio of 1:10 for evaluating the physiochemical properties of composting materials, respectively. Water extract was used to measure the matrix pH using a pH meter (OHAUS, China). A segmented flow analyser (Technicon Auto Analyser system, Germany) was used to quantify ammonium (NH_4^+), and nitrate (NO_3^-) contents in the composting piles using KCl extract.

2.3.2 Lignocellulose degradation and humification characteristics

The air-dried compost samples were ground to powder to determine lignocellulose composition and humification characteristics following methods previously reported by Vansoest et al. (1991) and Wang et al. (2021a), respectively. For lignocellulose composition analysis, powder samples were treated using neutral-detergent, followed by acid detergent and 72% sulphuric acid to obtain the content of neutral-detergent fibre (*NDF*, %), aciddetergent fibre (*ADF*, %), and acid-detergent lignin (*ADL*, %), respectively. The content of lignocellulose (%) in composting materials was then determined as:

$$Hemicellulose\ content = NDF - ADF \quad (1)$$

$$Cellulose\ content = ADF - ADL \quad (2)$$

$$Lignin\ content = ADL - Ash \quad (3)$$

where *Ash* was the ash content of composting materials (%), which was measured at the 550 °C in a muffle furnace for 5 h to remove organic matter as reported previously by Zhang et al. (2020). Lignocellulose degradation rate (R_d, %) was defined as follows:

$$R_d = \frac{m_0 - m_d}{m_0} \times 100\% \quad (4)$$

where m_0 and m_x were the contents of lignocellulose at the beginning and a sampling day (*d*) during composting, respectively.

Humic substances (HS) were extracted by blending powder samples with a solution of sodium hydroxide (0.1 M) and sodium pyrophosphate (0.1 M) at a mass ratio of 1:20 and then 24 h shaking at 20 °C. The HS extract was adjusted to pH 1 by adding 6 M hydrochloric acid to separate fulvic acid (FA) supernatant from humic acid (HA) precipitate. The HA precipitate was then dissolved in 0.1 M sodium hydroxide to obtain HA extract. HS, FA, and HA were quantified by measuring the total organic carbon (TOC) of their extracts using a TOC analyzer (TOC-V_{CSH}, Shimadzu, Kyoto). Ultraviolet-visible (UV-Vis) spectroscopy was also used to determine the specific ultraviolet absorbance at 280 nm ($SUVA_{280}$) for humification characterization after the

HS extract was diluted to the TOC concentration of 10 mg/L. The $SUVA_{280}$ is a representative spectroscopic index to evaluate HS structure in composting (Xu et al., 2021b).

2.3.3 Bacterial community analysis

Genomic DNA materials were extracted from compost samples on day 0, 7, and 35 for microbial community analysis using a method previously reported by Li et al. (2019a). Briefly, this method included genomic DNA extraction, polymerase chain reaction amplification of V3 – V4 regions, and high-throughput sequencing on the Illumina MiSeq platform (Illumina Inc., San Diego, CA, USA). Raw sequencing data were processed by Quantitative Insights into Microbial Ecology (QIIME 1.9.1). The optimized sequences were then clustered into operational taxonomy units (OTU) based on the 97% similarity level using the UPARSE pipeline. Ribosomal Database Project Classifier was then employed for taxonomic classification. All raw sequencing data were submitted to the Sequence Read Archive of the National Center for Biotechnology Information (NCBI) with the accession number PRJNA740163.

2.3.4 Statistical and network analysis

The Random Matrix Theory (RMT) based molecular ecological network analysis (MENA) was employed to construct modular network to decipher bacterial dynamics in relation to lignocellulose degradation, humification, and gaseous emissions in composting with and without lime addition. All network construction procedures followed the developer's recommendations on the online pipeline. Only the minimum number of members in each module was changed to 10 for modular network construction to achieve better visualization and discussion under high OTU coverage (> 85%). Moreover, the relationships between the modules with physiochemical properties, gaseous emissions, and humification were subsequently determined by the Mantel test to calculate the Euclidean distance matrix and OTU significance matrix.

3. Results and discussion

3.1 Effects of lime addition on composting performance

3.1.1 Physiochemical characteristics

All treatments showed the same temperature profile that was consistent with the sequential mesophilic, thermophilic, and mature stages of composting (Fig. 1A). All treatments achieved their temperature peaks on day 3. The composting temperature then gradually decreased with the depletion of readily biodegradable organic matter. Manual turning of composting piles could reallocate composting substrates and reactivate aerobic microbes (Yang et al., 2019). Thus, the temperature of all treatments increased again immediately after manual turning on day 7. From day 17 onward, the impact of manual turning on composting temperature was insignificant. All treatments entered into the mature stage as indicated by the continuous and gentle decrease in temperature to ambient condition.

Lime addition resulted in a clearly discernible impact on the temperature profile (Fig. 1A). The peak on day 3 was higher and the temperature remained higher with increasing lime dosage in the mesophilic and thermophilic composting stages. Then, treatments with lime addition showed lower temperature in the mature stages. In other words, lime addition accelerated the composting process. The observed acceleration could be attributed to the increased pH to improve the growth and activity of aerobic microbes for organic biodegradation (Onwosi et al., 2017). In addition, CaO in lime can react with water (moisture) to produce heat, thereby further promoting temperature increase.

All treatments showed a similar pH profile during composting (Fig. 1B). Kitchen waste is highly putrescible and can be hydrolyzed during transportation and storage to produce organic acids, resulting in the low pH at the beginning of composting (Xu et al., 2021a). During the composting process, organic acids are neutralized by NH_3, which is produced from mesophilic and thermophilic degradation of nitrogen bearing organic matter (Chan et al., 2016). It is noteworthy that the pH increase was more significant with increasing lime dosage as lime is a highly alkaline material.

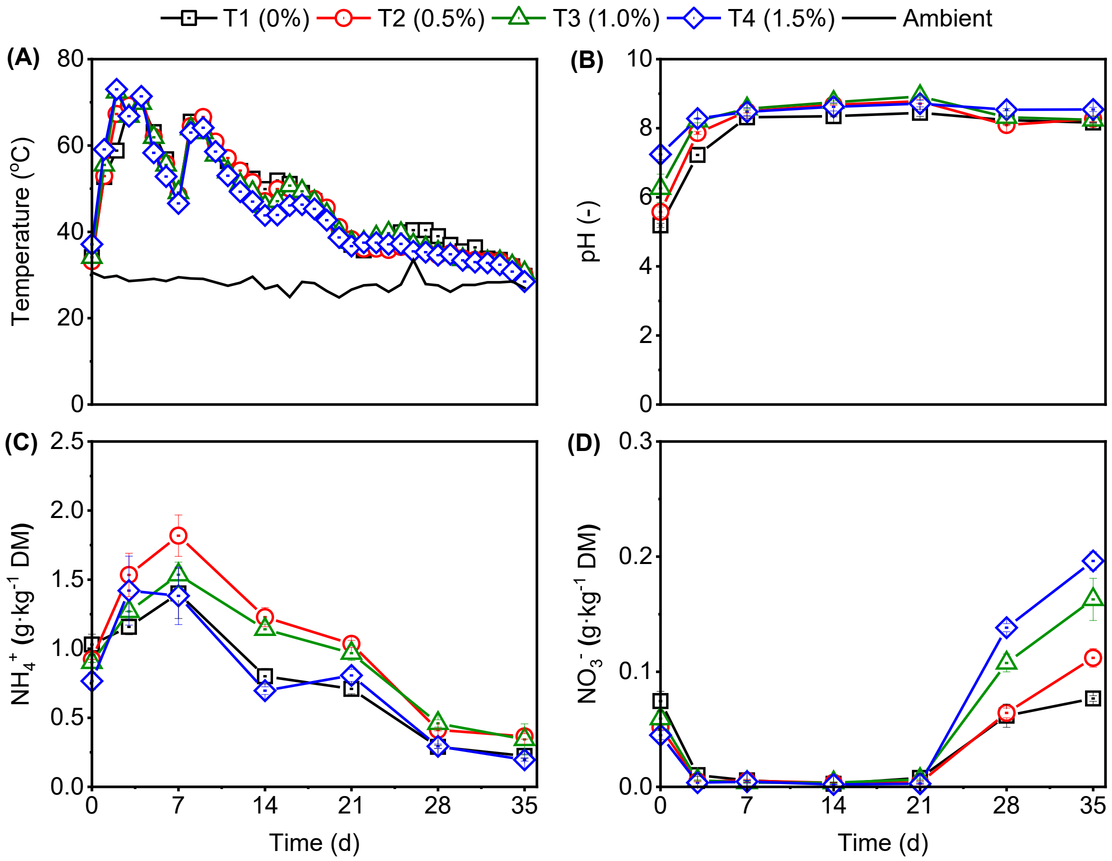

Fig. 1: (A) Temperature, (B) oxygen content, (C) matrix pH, (D) electrical conductivity, (E) ammonium nitrogen (NH_4^+), and (F) nitrate nitrogen (NO_3^-) during kitchen waste composting with different dosages of lime. Values shown in the parenthesis following each treatment were the addition proportion of lime on dry mass basis.

The NH_4^+ content in all treatments increased in the first week and decreased thereafter (Fig. 1C). The NH_4^+ increase was possibly due to the mineralization of organic nitrogen (e.g. protein and amino acids) and the thermophilic inhibition on nitrifiers (Wang et al., 2017). As the composting process progressed, the NH_4^+ content continuously declined from day 7 onward, given the continuous NH_3 emission at the thermophilic stage and the reactivated nitrification at the mature stage. Indeed, an increase in the NO_3^- content was observed for all treatments after manual turning on day 21 (Fig. 1D). Moreover, the increase in NO_3^- content was in the order of increasing lime dosage, possibly due to lime addition to improve the proliferation of nitrifiers (e.g. the family *Chitinophagaceae*).

It is noteworthy that the increase in NH_4^+ between day 7 and 21 due to lime addition was most significant at the low dosage of 0.5%. As the lime dosage increased, the increase in NH_4^+ production became less significant (Fig. 1C). This result was possibly due to the neutral reaction among $Ca(OH)_2$ and acid compounds to produce $CaCl_2$, which could chemically fix NH_3 as $CaCl_2 \cdot 8NH_3$ by complexation (Yamamoto et al., 1990).

3.1.2 Lignocellulose degradation and humification characteristics

Fig. 2 shows the impact of lime addition on lignocellulose degradation and humification. Hemicellulose and cellulose degradation occurred mostly during the thermophilic stage (Fig. 2A-B), whereas lignin degradation occurred most significantly during the mature stage. Compared to refractory lignin, hemicellulose and cellulose have more simple structure, thus, they can be easily biodegraded by thermophilic microbes in composting (Wei et al., 2019). An improvement in the hemicellulose, cellulose, and lignin degradation was observed for all treatments in the order of increasing lime addition (Fig. A-C). For example, the degradation of lignocellulose (i.e. hemicellulose, cellulose, and lignin) increased from 4.1% to 26.7% as lime content increased from 0.5% to 1.5%. This elevation could be ascribed to the improved matrix pH to facilitate the proliferation of functional microbes (e.g. thermophilic bacteria) for lignocellulose biodegradation (Zhu et al., 2021).

All treatments exhibited an increment and then decrease profiles in the FA content during composting (Fig. 2D). The initial increment was possibly due to the degradation of lignocellulose to form humus precursors and thus HS (i.e. HA and FA) (Zhang et al., 2019). However, FA could be employed as carbon resource for microbial metabolisms or polymerized to form stable HA with high aromatic carbon content (Duan et al., 2019). Thus, a continuous increase in HA content and $SUVA_{280}$ value was observed for all treatments during composting (Fig. 2E&F). Compared to the T1 treatment, the other treatments with lime addition notably improved the humification as indicated by their higher HA contents and $SUVA_{280}$ value. It has been reported that the lime addition could accelerate the hydrolysis of C-H bonds in lignocellulose to produce humus precursors during composting (Cai et al., 2019).

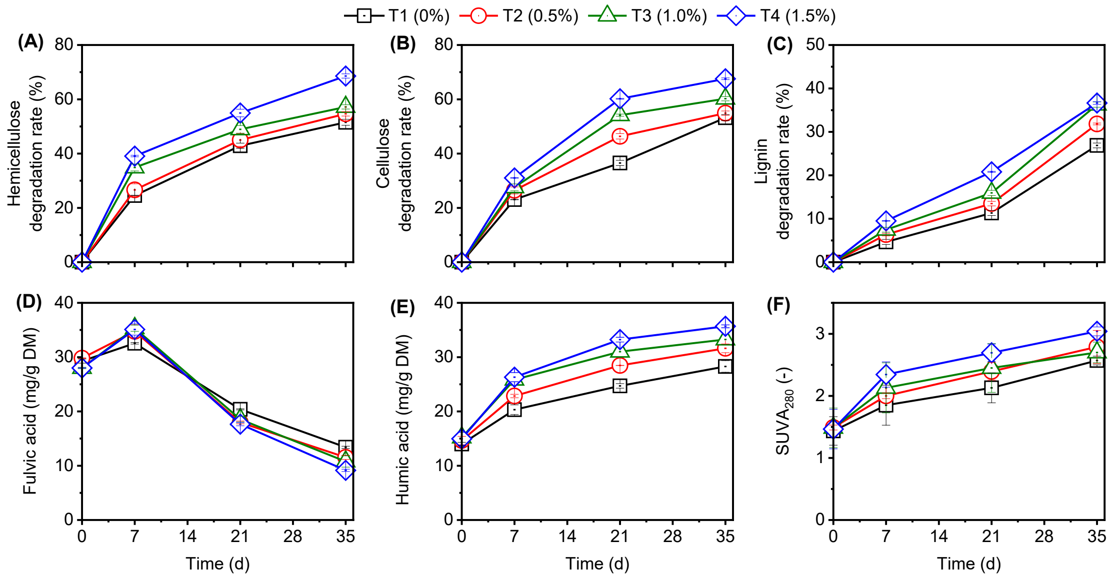

Fig. 2: Variations in the degradation rates of (A) hemicellulose, (B) cellulose, and (C) lignin as well as humification indexes, including (D) fulvic acid (FA), (E) humic acid (HA), and (F) $SUVA_{280}$ during kitchen waste composting with different dosages of lime.

3.1.3 Gaseous emissions

All treatments showed a similar CO_2 emission profile (Fig. 3A). CO_2 emission occurred mostly during the thermophilic stage due to organic mineralization. T2 – T4 treatments with lime addition had higher CO_2 emission in the initial stage and lower CO_2 emission at later stages. Thus, the accumulative CO_2 emissions of all treatments were similar at the end (Fig. 3B). This result could be attributed to the presence of neutral reaction between $Ca(OH)_2$ and CO_2 to generate $CaCO_3$ precipitation to promote carbon fixation in composting substrates.

CH_4 emission occurred mostly at the mesophilic and initial mature stages for all treatments (Fig. 3C). It has been reported that acidogenic and methanogenic bacteria could proliferate during the storage and transportation of kitchen waste due to its high moisture and organic contents (Xu et al., 2021a). Thus, all treatments exhibited a dramatic CH_4 emission at the beginning of composting. Given the inhibition of high temperature on methanogens and continuous aeration (Wen et al., 2021), the CH_4

emission of all treatments rapidly decreased to a negligible level from day 2 onward. With temperature reduction to mature stage after manual turning on day 14, the CH_4 emission emerged again for all treatments. Over the whole composting, the addition of lime slightly alleviated the accumulative CH_4 emission (Fig. 3D), possibly due to the increase matrix pH to facilitate the activities and growth of methanotrophs (Wang et al., 2021b).

N_2O emission occurred significantly during the mesophilic and mature stages for all treatments (Fig. 3E). The initial N_2O emission could be ascribed to the occurrence of anaerobic denitrifiers, such as the genus *Acinetobacter* and *Pseudomonas* that could transformed NO_3^- to nitrite (NO_2^-) and then N_2O (Song et al., 2020; Guo et al., 2021). With temperature increase to the thermophilic stage, most denitrifiers could be constricted to remarkably reduce N_2O emission (Yang et al., 2020). Given the temperature decrease to recover the activity of denitrifiers (Xu et al., 2021b), a more dramatic N_2O emission re-occurred for all treatments from day 21 onward. It is noted that both T3 and T4 treatments with lime addition higher than 1% could effectively reduce the N_2O accumulative emission by 26.3% (Fig. 3F). Such reduction was probably related to lime addition to inhibit the activities of denitrifiers and thus reduce NO_3^- availability (McMillan et al., 2016), as indicated by the increased NO_3^- content with an enhancement in lime dosage by the conclusion of composting (Fig. 1D).

All treatments reached to their peaks of NH_3 emission at the thermophilic stage (Fig. 3G). As reported previously, organic nitrogen could be mineralized to NH_4^+ and then NH_3 under high temperature and pH (Pagans et al., 2006). Given its improved organic mineralization and high temperature, the T2 and T3 treatments had a higher NH_3 accumulative emission in comparison with the T1 treatment (Fig. 3H). However, compared to the T1 treatment without lime addition, the T4 treatment with lime dosage at 1.5% reduced NH_3 emission by 25.9%, possibly owing to lime regulation of composting materials to drive ammonia fixation as $CaCl_2 \cdot 8NH_3$ as discussed above.

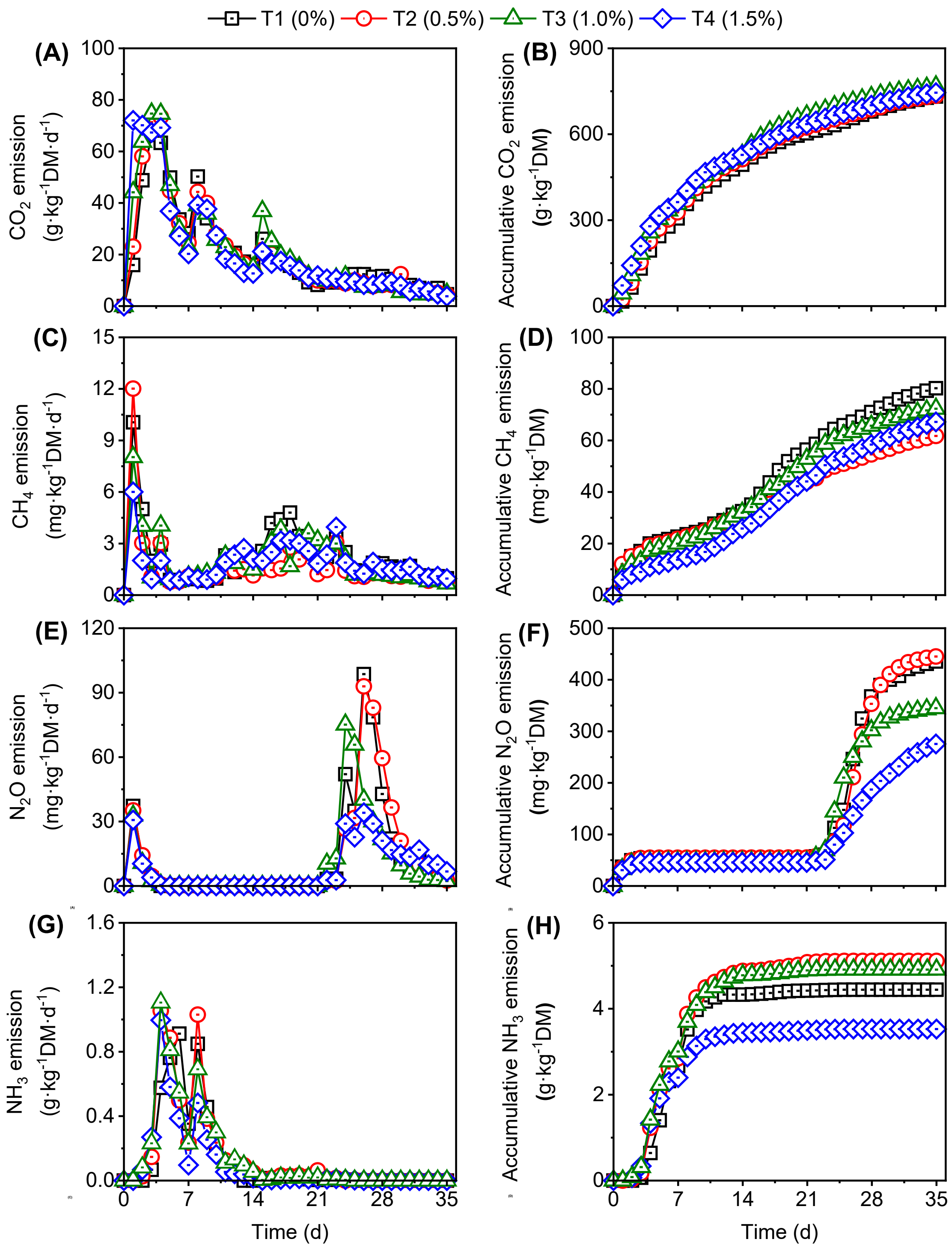

Fig. 3: (A) Daily CO_2 emission, (B) accumulative CO_2 emission, (C) daily CH_4 emission, (D) accumulative CH_4 emission, (E) daily N_2O emission, (F) accumulative N_2O emission, (G) daily NH_3 emission, and (H) accumulative NH_3 emission during kitchen waste composting with different dosages of lime.

3.2 Bacterial co-occurrence network analysis

3.2.1 Modular co-occurrence network analysis

The random matrix theory (RMT)-based co-occurrence network analysis was performed to modularize bacterial community for deciphering the underlying effects of lime addition on bacteria dynamics during composting (Fig.4 & Table 2). The constructed network has all fundamental topological characteristics, including scale-free, small-world, modularity. Specifically, the connectivity degree of all nodes in the network had an excellent fitting effect with the power-law model (R^2 = 0.92) to exhibit scale-free properties. Moreover, average clustering coefficient, path distance, and modularity of the empirical network were significantly higher than that of its corresponding random network under identical nodes and links, indicating its small-world behavior and modularity structure. As such, further analysis could be conducted given these qualified topological properties of the constructed network.

The OTU nodes in the network mainly affiliated to the phylum *Proteobacteria*, *Firmicutes*, *Actinobacteria*, *Bacteroidetes*, and *Chloroflexi* (Fig. 4), which have been identified as dominant contributors to drive composting process (Wei et al., 2018; Yin et al., 2019). Furthermore, the number of positive links was much more than that of negative links, suggesting the predominance of syntrophic and mutual relationships in the bacterial community during composting (Bello et al., 2020). On the other hand, the OTUs detected more than half of all samples were modularized using the greedy modularity optimization method. OTUs in each module were densely connected among one another and commonly possessed similar ecological functions or characteristics (Kong et al., 2019). Thus, each constituted module in the network can be regarded as a functional ecological niche to perform relevant activities at the different stage of composting.

Table 2: Major topological properties of empirical and random molecular ecological networks (MENs) of bacterial community in composting.

Empirical network							Random network		
R^2 of power law	Total nodes	Total links	Average degree	Average clustering coefficient	Average path distance	Modularity	Average clustering coefficient	Average path distance	Modularity
0.92	407	922	4.53	0.23	6.54	0.78	0.026 ± 0.005	3.82± 0.04	0.45± 0.01

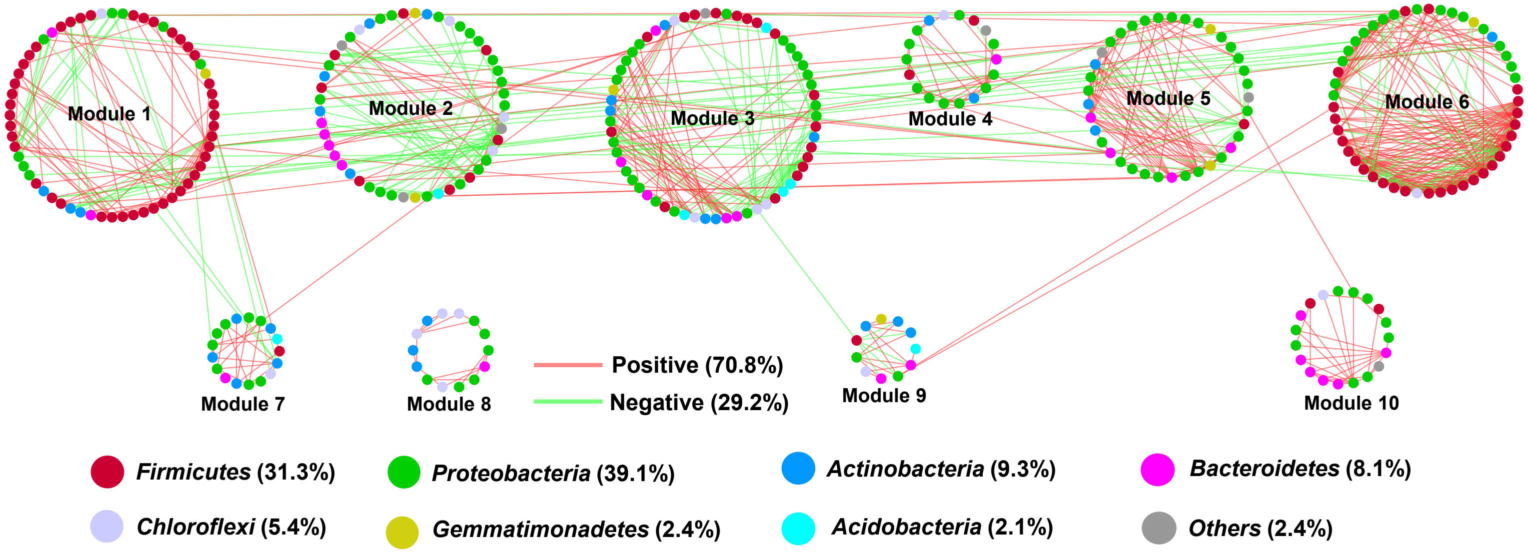

Fig. 4: Modularized co-occurrence network of bacterial community at the OTU level during kitchen waste composting. The formed modules with the nodes more than 10 were selected to construct final modularized co-occurrence network. The node colors represent different major phyla. Red and green lines represent positive and negative interactions, respectively.

3.2.2 Relationships between key modules and their major members

Eigengene network analysis was conducted to determine the relationships between key modules and thus unveiled higher-order organization in the constructed network (Fig. 5). All module eigengenes could explain 56% – 76% of total variation in the relative abundance of OTUs during composting. Such results indicate that these eigengenes could effectively represent the module profiles for eigengene network analysis. A shown in Fig. 5A, all modules were clustered into three meta-modules to display a higher-order organization based on their eigengene correlations. The three meta-modules mainly contained the representative OTUs at the mesophilic, thermophilic, and mature stages during composting, respectively (Fig. 5B – D).

Module 3, 6, 7, and 10 constructed the first meta-module, whose members mainly occurred at the mesophilic stage (Fig. 5B). Given their extremely low relative abundance (< 0.2%), all members of module 10 were not visualized for further analysis. The first meta-module was dominated by the anaerobic acidogens, mainly including members belonged to the genus *Lactobacillus* (e.g. *the species Lactobacillus fermentum*, *Lactobacillus alimentarius*, and *Lactobacillus plantarum*), and *the species Lactococcus lactis*, possibly due to their proliferation during the storage and transportation of kitchen waste. These acidogens could produce massive organic acids to contribute to the low matrix pH and thus CH_4 production (Xu et al., 2021c). Moreover, several denitrifiers, such as the genus *Hyphomicrobium*, and *Acinetobacter* as well as its affiliated species, also considerably occurred to use nitrite and nitrate as electron acceptor to trigger N_2O emission at the mesophilic stage (Song et al., 2020). On the other hand, kitchen waste storage promoted the breeding of pathogenic bacteria, including the family *Enterobacteriaceae*, the genus *Escherichia-Shigella*, and the species *Weissella confuse* (Aberkane et al., 2017; Colavecchio et al., 2017). It is noteworthy that the relative abundance of most bacteria in this meta-module obviously decreased when lime dosage increased to 1.0%. Indeed, it has been reported that lime addition could effectively inactivate microbes through damaging their outer membrane and nucleic acid before composting (Hijikata et al., 2016).Thus, such inactivation mechanism could be another contributor for the relatively lower emission of CH_4 and N_2O at the mesophilic stage of the T3 and T4 treatments with higher lime addition.

As composting temperature increased to the thermophilic stage, most thermophilic bacteria became predominant to enrich in module 1 as the second meta-module (Fig. 5C). Almost all of these thermophilic bacteria subordinated to the phylum *Firmicutes* that were thermotolerant and could be responsible for the biodegradation of organic substances, such as lignocellulose and protein (Liu et al., 2018). Compared to the T1 treatment, the other treatments with lime addition remarkably increased the relative abundance of the family *Limnochordaceae* and *Thermoactinomycetaceae*, as well as the genus *Brevibacillus*, *Paenibacillus*, *Planifilum*, and *Sinibacillus*. It has been reported that the family *Thermoactinomycetaceae* could secrete dehydrogenase and polyphenol oxidase to decompose cellulose and soluble lignin at the thermophilic stage of composting (Ke et al., 2010; Arab et al., 2017). Furthermore, the genus *Planifilum*, *Sinibacillus*, and *Paenibacillus* could biodegrade macromolecular organic substances (e.g. lignocellulose) into micromolecular humus precursors for further humus polymerization (Zhu et al., 2021). As such, lime addition improved the lignocellulose degradation efficiencies and humification at the thermophilic stage. Despite its higher relative abundance of thermophilic bacteria for organic biodegradation, the T4 treatment exhibited a lower NH_3 emission throughout composting in comparison with other treatments. This result further verified that abiotic process (i.e. chemical reactors between $CaCl_2$ and NH_3) could be a dominant pathway to reduce NH_3 emission.

The main bacteria at the mature stage were distributed into module 2, module 4, module 5, module 8, and module 9 (Fig. 5D), all of which formed the third meta-module and involved in the biodegradation of refractory compounds and denitrification (Maeda et al., 2018; Xu et al., 2021b). The relative abundance of the order *Xanthomonadales*, the family *Cytophagaceae*, the genus *Steroidobacter*, *Roseiflexus*, and *Nonomuraea* in this meta-module gradually declined in response to an increment in the lime contents. Of these declined bacteria, the order *Xanthomonadales* and the genus *Steroidobacter* have been identified as denitrifiers (Maeda et al., 2018), which were probably inhibited under high lime content circumstance (> 6 tonne lime ha^{-1}) (Suzuki et al., 2021; Wang et al., 2021b). Thus, relatively low N_2O emission was observed for the T3 and T4 treatments with lime addition after the thermophilic stage. Moreover, lime addition also facilitated the proliferation of the family *Chitinophagaceae*, the genus *Cellvibrio*, *Pseudomonas*, and *Ruminofilibacter*. These bacteria genera could transform persistent lignocellulose into humus precursors (Yin et al., 2019). Moreover, the family *Chitinophagaceae* as heterotrophic ammonia oxidizing bacteria could promote the NO_3^- formation (Wang et al., 2020). These results demonstrate that lime amendment could effectively enrich functional bacteria to enhance humification and NO_3^- content and meanwhile restrict acidogens and denitrifiers to reduce GHG emissions, thereby improving compost quality.

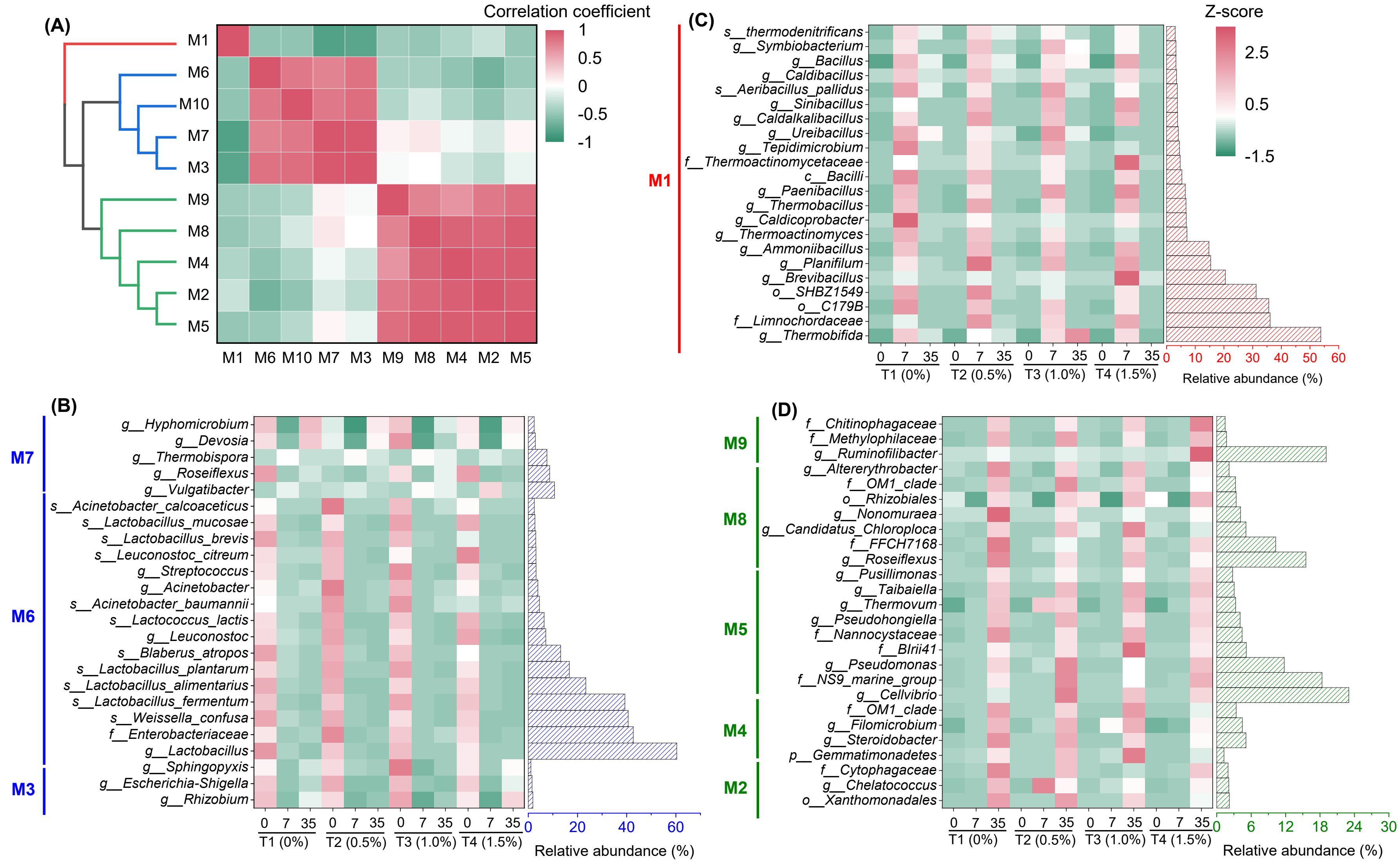
(A)
Correlation coefficient
1
0.5
0
-0.5
-1
M1
M6
M10
M7
M3
M9
M8
M4
M2
M5
(B)
M7
M6
M3
g__Hyphomicrobium
g__Devosia
g__Thermobispora
g__Roseiflexus
g__Vulgatibacter
s__Acinetobacter_calcoaceticus
s__Lactobacillus_mucosae
s__Lactobacillus_brevis
s__Leuconostoc_citreum
g__Streptococcus
g__Acinetobacter
s__Acinetobacter_baumannii
s__Lactococcus_lactis
g__Leuconostoc
s__Blaberus_atropos
s__Lactobacillus_plantarum
s__Lactobacillus_alimentarius
s__Lactobacillus_fermentum
s__Weissella_confusa
f__Enterobacteriaceae
g__Lactobacillus
g__Sphingopyxis
g__Escherichia-Shigella
g__Rhizobium
0 7 35 0 7 35 0 7 35 0 7 35
T1 (0%) T2 (0.5%) T3 (1.0%) T4 (1.5%)
0 20 40 60
Relative abundance (%)
(C)
M1
s__thermodenitrificans
g__Symbiobacterium
g__Bacillus
g__Caldibacillus
s__Aeribacillus_pallidus
g__Sinibacillus
g__Caldalkalibacillus
g__Ureibacillus
g__Tepidimicrobium
f__Thermoactinomycetaceae
c__Bacilli
g__Paenibacillus
g__Thermobacillus
g__Caldicoprobacter
g__Thermoactinomyces
g__Ammoniibacillus
g__Planifilum
g__Brevibacillus
o__SHBZ1549
o__C179B
f__Limnochordaceae
g__Thermobifida
Z-score
2.5
0.5
-1.5
0 7 35 0 7 35 0 7 35 0 7 35
T1 (0%) T2 (0.5%) T3 (1.0%) T4 (1.5%)
0 10 20 30 40 50 60
Relative abundance (%)
(D)
M9
M8
M5
M4
M2
f__Chitinophagaceae
f__Methylophilaceae
g__Ruminofilibacter
g__Altererythrobacter
f__OM1_clade
o__Rhizobiales
g__Nonomuraea
g__Candidatus_Chloroploca
f__FFCH7168
g__Roseiflexus
g__Pusillimonas
g__Taibaiella
g__Thermovum
g__Pseudohongiella
f__Nannocystaceae
f__BIrii41
g__Pseudomonas
f__NS9_marine_group
g__Cellvibrio
f__OM1_clade
g__Filomicrobium
g__Steroidobacter
p__Gemmatimonadetes
f__Cytophagaceae
g__Chelatococcus
o__Xanthomonadales
0 7 35 0 7 35 0 7 35 0 7 35
T1 (0%) T2 (0.5%) T3 (1.0%) T4 (1.5%)
0 6 12 18 24 30
Relative abundance (%)

450

Fig. 5: Relationships between key modules (A) and their major members (relative abundance > 1%) at the OTU level (B – D) in the co-occurrence network. In the Fig. 5A, the left part shows the hierarchical clustering based on the Pearson correlations among module eigengenes and the right heatmap is their coefficient values. In Fig. 5B – D, the color key represents OTU as standard score (z-score).

3.2.3 Correlations between main modules with physiochemical properties, gaseous emissions and humification

The relationships between main modules with physiochemical properties, gaseous emissions, and humification were established by the Mantel test to further reveal the improved composting performance in response to lime addition (Fig. 6). In the first meta-module, module 3 and 6 were significantly positive with CH_4 and N_2O emissions, but negative with matrix pH. As discussed above, most members in both modules were acidogens, methanogens, and denitrifiers, which readily resulted in matrix acidification to reduce matrix pH and produced massive GHGs under oxygen deficiency condition. Similarly, module 7 also exhibited an adverse relationship with the matrix pH in composting. These results suggest that adding lime could increase the matrix pH to inhibit the activities and growth of anaerobic bacteria at the mesophilic stage, thus reducing GHG emission at the beginning of composting. Indeed, a negative association was observed between the matrix pH with the CH_4 and N_2O emissions.

Module 1 had a significantly positive correlation with temperature, pH, NH_4^+, CO_2, NH_3, and lignocellulose degradation (Fig. 6), possibly due to its enrichment of thermophilic bacteria for rapid organic biodegradation and mineralization at the thermophilic stage (Ke et al., 2010; Arab et al., 2017; Liu et al., 2018). It is noted that the correlation coefficients of lignocellulose degradation ($R^2 < 0.80$) were relatively lower than that of other parameters ($R^2 > 0.80$). This result could be ascribed to the fact that organic mineralization for the production of NH_4^+, CO_2, and NH_3 mainly appeared at the thermophilic stage while the lignocellulose biodegradation was a continuous process over composting. The significantly positive correlations were also observed for matrix pH and CO_2, NH_3, lignocellulose degradation, and humification. Moreover, adding lime could enhance the relative abundance of thermophilic bacteria, such as the family *Thermoactinomycetaceae* and the genus *Brevibacillus*, as discussed above. Thus, the lime amelioration was probably caused by increased pH to strengthen the proliferation of thermophilic bacteria for lignocellulose decomposition and humification at the thermophilic stage.

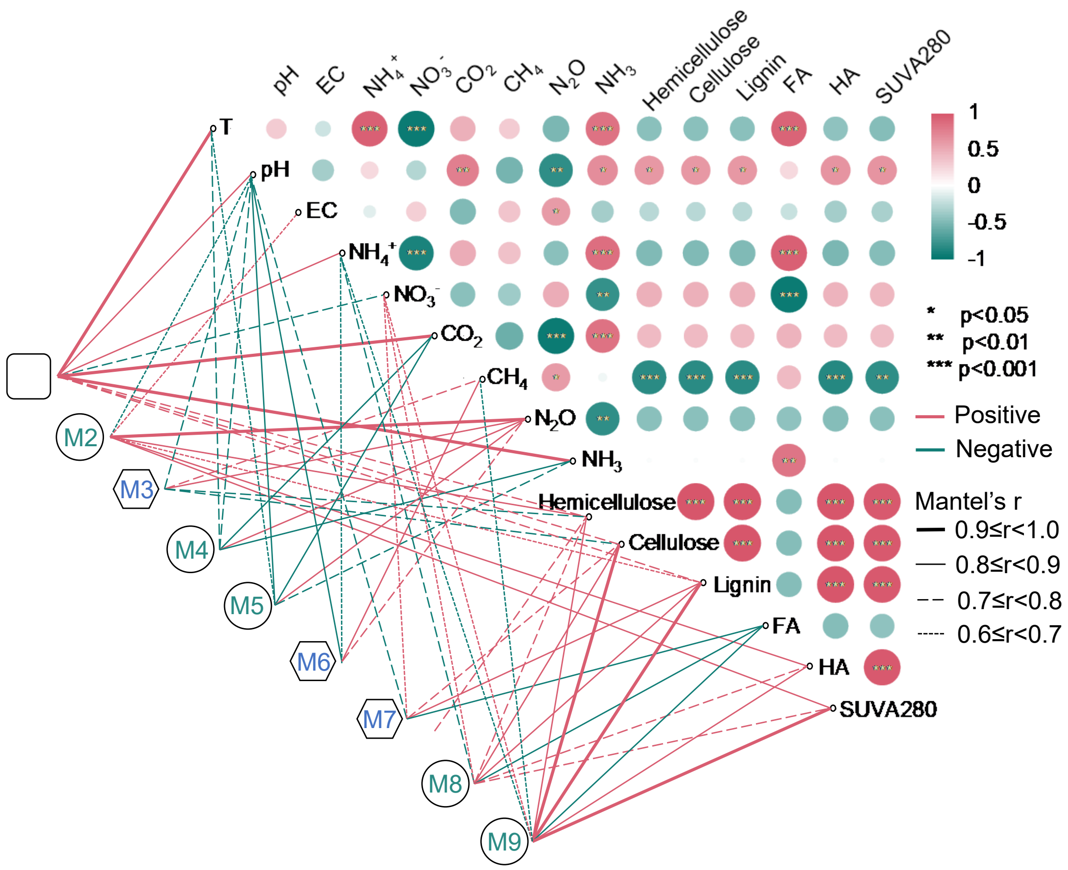

Fig. 6: Correlation between network modules with physiochemical properties, gaseous emissions and humification. Pairwise comparisons of physiochemical properties, gaseous emissions and humification are shown in the heatmap with a color gradient to represent Spearman's correlation coefficients. Statistically significant correlations between network modules with physiochemical properties, gaseous emissions and humification determined by the Mantel test are shown in the lower-left. Edge width corresponds to the Mantel's coefficients. Red and green lines represent positive and negative interactions, respectively.

0

4. Conclusion

Results from this study demonstrate that lime could regulate both biotic and abiotic processes to improve kitchen waste composting. Modular network analysis deciphered that acidogens and denitrifiers as dominant bacteria in the mesophilic stage were suppressed by lime to reduce GHG emission. Lime addition also enhanced matrix pH and temperature via hydrogen reaction to proliferate thermophilic bacteria (e.g. *Thermoactinomycetaceae* and *Planifilum*) for organic biodegradation and then humification. In the mature stage, lime inhibited denitrifiers but enriched nitrifiers to reduce N_2O emission and facilitate NO_3^- formation, respectively. Moreover, lime addition at 1.5% exhibited chemical fixation to reduce NH_3 emission.

5. Acknowledgements

This research was supported under the National Key R&D Program of China (No. 2018YFC1901000).

6. References

[1] Aberkane, S., Didelot, M.N., Carriere, C., Laurens, C., Sanou, S., Godreuil, S., Jean-Pierre, H. 2017. Weissella confusa bacteremia: An underestimated opportunistic pathogen. *Med Maladies Infect*, **47**(4), 297-299.

[2] Arab, G., Razaviarani, V., Sheng, Z.Y., Liu, Y., McCartney, D. 2017. Benefits to decomposition rates when using digestate as compost co-feedstock: Part II - Focus on microbial community dynamics. *Waste Manage*, **68**, 85-95.

[3] Bello, A., Han, Y., Zhu, H., Deng, L., Yang, W., Meng, Q., Sun, Y., Egbeagu, U.U., Sheng, S., Wu, X., Jiang, X., Xu, X. 2020. Microbial community composition, co-occurrence network pattern and nitrogen transformation genera response to biochar addition in cattle manure-maize straw composting. *Sci Total Environ*, **721**, 137759.

[4] Cai, Y.Y., He, Y.H., He, K., Gao, H.J., Ren, M.J., Qu, G.F. 2019. Degradation mechanism of lignocellulose in dairy cattle manure with the addition of calcium oxide and superphosphate. *Environ Sci Pollut R*, **26**(32), 33683-33693.

[5] Chan, M.T., Selvam, A., Wong, J.W.C. 2016. Reducing nitrogen loss and salinity

during 'struvite' food waste composting by zeolite amendment. *Bioresour Technol*, **200**, 838-844.

[6] Chen, Z.Q., Fu, Q.Q., Cao, Y.S., Wen, Q.X., Wu, Y.Q. 2021. Effects of lime amendment on the organic substances changes, antibiotics removal, and heavy metals speciation transformation during swine manure composting. *Chemosphere*, **262**.

[7] Cheng, H., Li, Y.M., Li, L., Chen, R., Li, Y.Y. 2020. Long-term operation performance and fouling behavior of a high-solid anaerobic membrane bioreactor in treating food waste. *Chem Eng J*, **394**.

[8] Colavecchio, A., Cadieux, B., Lo, A., Goodridge, L.D. 2017. Bacteriophages Contribute to the Spread of Antibiotic Resistance Genes among Foodborne Pathogens of the Enterobacteriaceae Family - A Review. *Front Microbiol*, **8**.

[9] Deng, Y., Jiang, Y.H., Yang, Y.F., He, Z.L., Luo, F., Zhou, J.Z. 2012. Molecular ecological network analyses. *Bmc Bioinformatics*, **13**.

[10] Ding, Y., Wei, J.J., Xiong, J.S., Zhou, B.W., Cai, H.J., Zhu, W.Q., Zhang, H.J. 2019. Effects of operating parameters on in situ NH_3 emission control during kitchen waste composting and correlation analysis of the related microbial communities. *Environ Sci Pollut R*, **26**(12), 11756-11766.

[11] Duan, Y.M., Awasthi, S.K., Liu, T., Zhang, Z.Q., Awasthi, M.K. 2019. Response of bamboo biochar amendment on volatile fatty acids accumulation reduction and humification during chicken manure composting. *Bioresour Technol*, **291**.

[12] Fernandez-Gonzalez, A.J., Cardoni, M., Gomez-Lama Cabanas, C., Valverde-Corredor, A., Villadas, P.J., Fernandez-Lopez, M., Mercado-Blanco, J. 2020. Linking belowground microbial network changes to different tolerance level towards Verticillium wilt of olive. *Microbiome*, **8**(1).

[13] Guo, H.H., Gu, J., Wang, X.J., Song, Z.L., Nasir, M., Tuo, X.X. 2021. Elucidating the microbiological characteristics of cyromazine affecting the nitrogen cycle during aerobic composting of pig manure. *Sci Total Environ*, **764**.

[14] Hijikata, N., Tezuka, R., Kazama, S., Otaki, M., Ushijima, K., Ito, R., Okabe, S., Sano, D., Funamizu, N. 2016. Bactericidal and virucidal mechanisms in the alkaline disinfection of compost using calcium lime and ash. *J Environ Manage*, **181**, 721-727.

[15] Jiang, Y., Sun, B., Li, H., Liu, M., Chen, L., Zhou, S. 2015. Aggregate-related changes in network patterns of nematodes and ammonia oxidizers in an acidic soil. *Soil Biol Biochem*, **88**, 101-109.

[16] Ke, G.R., Lai, C.M., Liu, Y.Y., Yang, S.S. 2010. Inoculation of food waste with the thermo-tolerant lipolytic actinomycete Thermoactinomyces vulgaris A31 and maturity evaluation of the compost. *Bioresour Technol*, **101**(19), 7424-7431.

[17] Kong, Z.Y., Wu, Z.J., Glick, B.R., He, S.Y., Huang, C., Wu, L. 2019. Co-occurrence patterns of microbial communities affected by inoculants of plant growth-promoting bacteria during phytoremediation of heavy metal contaminated soils. *Ecotoxicology and Environmental Safety*, **183**.

[18] Li, J., Wang, T., Yu, S., Bai, J., Qin, S. 2019a. Community characteristics and ecological roles of bacterial biofilms associated with various algal settlements on coastal reefs. *J Environ Manage*, **250**.

[19] Li, Y., Cui, S., Chang, S.X., Zhang, Q.P. 2019b. Liming effects on soil pH and crop yield depend on lime material type, application method and rate, and crop species: a global meta-analysis. *J Soil Sediment*, **19**(3), 1393-1406.

[20] Liu, L., Wang, S.Q., Guo, X.P., Zhao, T.N., Zhang, B.L. 2018. Succession and diversity of microorganisms and their association with physicochemical properties during green waste thermophilic composting. *Waste Manage*, **73**, 101-112.

[21] Maeda, K., Miyatake, F., Asano, R., Nakajima, K., Maeda, T., Iwabuchi, K. 2018. Response of the denitrifier community and its relationship with multiple N2O emission peaks after mature compost addition into dairy manure compost with forced aeration. *Chemosphere*, **206**, 310-319.

[22] McMillan, A.M.S., Pal, P., Phillips, R.L., Palmada, T., Berben, P.H., Jha, N., Saggar, S., Luo, J.F. 2016. Can pH amendments in grazed pastures help reduce N_2O emissions from denitrification? - The effects of liming and urine addition on the completion of denitrification in fluvial and volcanic soils. *Soil Biol Biochem*, **93**, 90-104.

[23] Nghiem, L.D., Koch, K., Bolzonella, D., Drewes, J.E. 2017. Full scale co-digestion of wastewater sludge and food waste: Bottlenecks and possibilities. *Renew Sust Energ Rev*, **72**, 354-362.

[24] Onwosi, C.O., Igbokwe, V.C., Odimba, J.N., Eke, I.E., Nwankwoala, M., Iroh, I.N., Ezeogu, L.I. 2017. Composting technology in waste stabilization: On the methods, challenges and future prospects. *J Environ Manage*, **190**, 140-157.

[25] Pagans, E., Barrena, R., X, F., Sanchez, A. 2006. Ammonia emissions from the composting of different organic wastes. Dependency on process temperature. *Chemosphere*, **62**(9), 1534-1542.

[26] Singh, J., Kalamdhad, A.S. 2013. Effects of lime on bioavailability and leachability of heavy metals during agitated pile composting of water hyacinth. *Bioresour Technol*, **138**, 148-155.

[27] Song, J., Li, Q., Dzakpasu, M., Wang, X.C.C., Chang, N.N. 2020. Integrating stereo-elastic packing into ecological floating bed for enhanced denitrification in landscape water. *Bioresour Technol*, **299**.

[28] Suzuki, K., Kashiwa, N., Nomura, K., Asiloglu, R., Harada, N. 2021. Impacts of application of calcium cyanamide and the consequent increase in soil pH on N2O emissions and soil bacterial community compositions. *Biol Fert Soils*, **57**(2), 269-279.

[29] Vansoest, P.J., Robertson, J.B., Lewis, B.A. 1991. Methods for Dietary Fiber, Neutral Detergent Fiber, and Nonstarch Polysaccharides in Relation to Animal Nutrition. *J Dairy Sci*, **74**(10), 3583-3597.

[30] Wang, Q., Awasthi, M.K., Ren, X.N., Zhao, J.C., Li, R.H., Wang, Z., Chen, H.Y.,

Wang, M.J., Zhang, Z.Q. 2017. Comparison of biochar, zeolite and their mixture amendment for aiding organic matter transformation and nitrogen conservation during pig manure composting. *Bioresour Technol*, **245**, 300-308.

[31] Wang, W., Hou, Y., Huang, W., Liu, X., Wen, P., Wang, Y., Yu, Z., Zhou, S. 2021a. Alkali lignin and sodium lignosulfonate additives promote the formation of humic substances during paper mill sludge composting. *Bioresour Technol*, **320**(Pt A), 124361.

[32] Wang, Y., Yao, Z.S., Zhan, Y., Zheng, X.H., Zhou, M.H., Yan, G.X., Wang, L., Werner, C., Butterbach-Bahl, K. 2021b. Potential benefits of liming to acid soils on climate change mitigation and food security. *Global Change Biol*, **27**(12), 2807-2821.

[33] Wang, Z.Y., Yao, Y.U., Steiner, N., Cheng, H.H., Wu, Y.J., Woo, S.G., Criddle, C.S. 2020. Impacts of nitrogen-containing coagulants on the nitritation/denitrification of anaerobic digester centrate. *Environ Sci Water Res Technol*, **6**(12), 3451-3459.

[34] Wei, H.W., Wang, L.H., Hassan, M., Xie, B. 2018. Succession of the functional microbial communities and the metabolic functions in maize straw composting process. *Bioresour Technol*, **256**, 333-341.

[35] Wei, Y.Q., Wu, D., Wei, D., Zhao, Y., Wu, J.Q., Xie, X.Y., Zhang, R.J., Wei, Z.M. 2019. Improved lignocellulose-degrading performance during straw composting from diverse sources with actinomycetes inoculation by regulating the key enzyme activities. *Bioresour Technol*, **271**, 66-74.

[36] Wen, P., Tang, J., Wang, Y.Q., Liu, X.M., Yu, Z., Zhou, S.G. 2021. Hyperthermophilic composting significantly decreases methane emissions: Insights into the microbial mechanism. *Sci Total Environ*, **784**.

[37] Xiong, X.N., Yu, I.K.M., Tsang, D.C.W., Bolan, N.S., Ok, Y.S., Igalavithana, A.D., Kirkham, M.B., Kim, K.H., Vikrant, K. 2019. Value-added chemicals from food supply chain wastes: State-of-the-art review and future prospects. *Chem Eng*

J, **375**.

[38] Xu, Z., Ma, Y., Zhang, L., Han, Y., Yuan, J., Li, G., Luo, W. 2021a. Relating bacterial dynamics and functions to gaseous emissions during composting of kitchen and garden wastes. *Sci Total Environ*, **767**, 144210-144210.

[39] Xu, Z., Qi, C., Zhang, L., Ma, Y., Li, J., Li, G., Luo, W. 2021b. Bacterial dynamics and functions for gaseous emissions and humification in response to aeration intensities during kitchen waste composting. *Bioresour Technol*, **337**, 125369.

[40] Xu, Z., Xu, W., Zhang, L., Ma, Y., Li, Y., Li, G., Nghiem, L.D., Luo, W. 2021c. Bacterial dynamics and functions driven by bulking agents to mitigate gaseous emissions in kitchen waste composting. *Bioresour Technol*, **332**, 125028.

[41] Yamamoto, H., Sakamoto, Y., Sanga, S., Tokunaga, J. 1990. Performance of Thermal-Energy Storage Unit Using $CaCl_2$-NH_3 System Mixed with Ti. *Can J Chem Eng*, **68**(6), 948-951.

[42] Yang, F., Li, G.X., Yang, Q.Y., Luo, W.H. 2013. Effect of bulking agents on maturity and gaseous emissions during kitchen waste composting. *Chemosphere*, **93**(7), 1393-1399.

[43] Yang, F., Li, Y., Han, Y.H., Qian, W.T., Li, G.X., Luo, W.H. 2019. Performance of mature compost to control gaseous emissions in kitchen waste composting. *Sci Total Environ*, **657**, 262-269.

[44] Yang, Y.J., Awasthi, M.K., Wu, L.L., Yan, Y., Lv, J.L. 2020. Microbial driving mechanism of biochar and bean dregs on NH_3 and N_2O emissions during composting. *Bioresour Technol*, **315**.

[45] Yin, Y.A., Gu, J., Wang, X.J., Zhang, Y.J., Zheng, W., Chen, R., Wang, X.C. 2019. Effects of rhamnolipid and Tween-80 on cellulase activities and metabolic functions of the bacterial community during chicken manure composting. *Bioresour Technol*, **288**.

[46] Zhang, D.F., Xu, Z.C., Wang, G.Y., Huda, N., Li, G.X., Luo, W.H. 2020. Insights

into characteristics of organic matter during co-biodrying of sewage sludge and kitchen waste under different aeration intensities. *Environ Technol Inno*, **20**.

[47] Zhang, Z.C., Zhao, Y., Yang, T.X., Wei, Z.M., Li, Y.J., Wei, Y.Q., Chen, X.M., Wang, L.Q. 2019. Effects of exogenous protein-like precursors on humification process during lignocellulose-like biomass composting: Amino acids as the key linker to promote humification process. *Bioresour Technol*, **291**.

[48] Zhao, X.Y., Tan, W.B., Dang, Q.L., Li, R.F., Xi, B.D. 2019. Enhanced biotic contributions to the dechlorination of pentachlorophenol by humus respiration from different compostable environments. *Chem Eng J*, **361**, 1565-1575.

[49] Zhu, N., Gao, J., Liang, D., Zhu, Y.Y., Li, B.Q., Jin, H.M. 2021. Thermal pretreatment enhances the degradation and humification of lignocellulose by stimulating thermophilic bacteria during dairy manure composting. *Bioresour Technol*, **319**.